Manufacturing Letters 45 (2025) 88–92

Contents lists available at ScienceDirect

Manufacturing Letters

journal homepage: www.elsevier.com/locate/mfglet

Letters

Rapid prototyping of microfluidic multi-scale lab-on-a-foil devices in COC

Salman Murad [a], Marvin Heyer [a], Fabian Lickert [b], Judith Schlanderer [b], Daniel Kainz [b], Markus Rombach [a,b], Christoph Stöver [c], Thomas Ruhl [c], Benedikt Bläsi [d], Julian Menges [b], Tobias Hutzenlaub [a,b], Nils Paust [a,b], Peter Juelg [a,b,*]

[a] Laboratory for MEMS Applications, IMTEK-Department of Microsystems Engineering, University of Freiburg, Freiburg, Germany
[b] Hahn-Schickard, Freiburg, Germany
[c] Temicon GmbH, Dortmund, Germany
[d] Fraunhofer Institute for Solar Energy Systems, Freiburg, Germany

ARTICLE INFO

Article history:
Received 27 March 2025
Received in revised form 14 July 2025
Accepted 24 July 2025
Available online 30 July 2025

Keywords:
Rapid prototyping
COC film
Microstructures
Nanostructures
Microfluidics

ABSTRACT

Developing scalable and cost-effective fabrication methods for microfluidic lab-on-a-chip devices is critical to bridging the gap between rapid prototyping and mass production. We present a rapid and affordable prototyping method for lab-on-a-foil devices with multi-scale fluidic features ranging from picoliters (features size: 20 μm) to microliters (feature size: 100–1500 μm). Our three-step approach — thermoforming, hot embossing, and thermal sealing — enables the co-integration of picoliter wells with nano- to microliter channels and chambers using cyclic olefin copolymer (COC), a thermoplastic polymer suitable for scalable manufacturing without requiring additional surface treatments. This method overcomes the limitations of non-scalable polydimethylsiloxane (PDMS) prototyping and the high initial cost of thermoplastic injection molding. With low tooling costs, rapid turnaround times, and material compatibility with high-precision mass production, this technique offers an efficient pathway for the development of multi-scale lab-on-a-chip devices for applications such as digital PCR and solid phase extraction.

1. Introduction

Lab-on-a-chip applications can require integration of pico- to microliter features in one device, termed as multi-scale, e.g. for methods like digital polymerase chain reaction (dPCR) [1–3], solid phase extraction [4,5] or chromatography columns [6]. Combining pico- to microliter features in one device enables combination of macroscopic sample preparation structures with highly-integrated and miniaturized analysis structures. Current replication techniques merging tools from lithography (for picoliter patterns) and micro-milling (for microliter features) often rely on expensive or non-scalable materials like silicon [7] or polydimethylsiloxane (PDMS) [1,8,9]. These limitations can lead to undesired material changes during next stages of product development, posing a risk to the functionality of the microfluidic chip. Alternatively, multi-scale devices can be fabricated by injection molding [2,10,11]. However, injection molding has too high lead time and initial tooling cost to be applied for rapid prototyping. 3D printing, such as fused deposition modelling (FDM) can provide rapid and low-cost prototyping, however, the limited resolution still limits its widespread use for microfluidics. Film-based polymer replication, known as lab-on-a-foil, presents a solution for rapid, low-cost prototyping with thermoplastic film materials such as cyclic olefin copolymer (COC) [12,13]. However, existing lab-on-a-foil devices have focused primarily on the micro- to nanoliter range [5,14–17]. This paper introduces a prototyping method for integrating pico- to microliter features into COC lab-on-a-foil devices using a three-step process.

2. Materials and methods

2.1. Fabrication concept

The three-step fabrication process (Fig. 1) allows for the decoupling of feature sizes in a multi-scale device. It utilizes a co-extruded COC film, made of a low melting layer (20 μm, COC 8007) and a high melting layer (180 μm, COC 6013).

* Corresponding author at: Laboratory for MEMS Applications, IMTEK-Department of Microsystems Engineering, University of Freiburg, Freiburg, Germany.
E-mail address: Peter.Juelg@Hahn-Schickard.de (P. Juelg).

https://doi.org/10.1016/j.mfglet.2025.07.005
2213-8463/

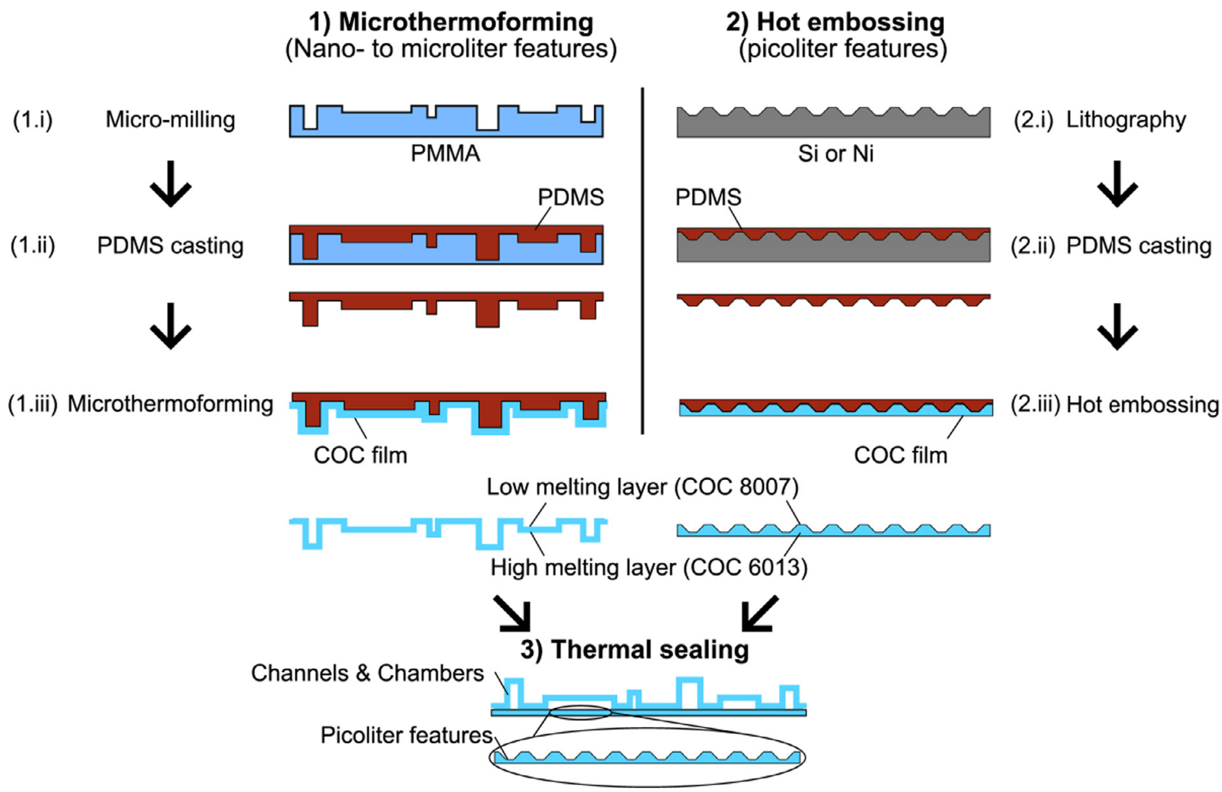

Fig. 1. Fabrication process: 1.) Replication of milled nano- to microliter features *via* microthermoforming in COC film. 2.) Replication of picoliter features from lithography *via* hot embossing into a second COC film. 3.) Both COC films bonded *via* thermal sealing.

Step 1: Microfluidic channels and chambers (nano- to microliter features) and world-to-chip interfaces (e.g. inlet ports and vents) are fabricated using microthermoforming of a COC film [18,19]. For this purpose, a microfluidic CAD model (SolidWorks, Dassault Systèmes) is transferred into a polymethyl-methacrylate (PMMA) plate by micro-milling (EVO, KERN Microtechnik) to create a negative master. Based on the PMMA plate a positive master is cast in PDMS (Elastosil RT-607, Wacker Chemie). It is important to note that the PDMS master should be renewed after 20 COC film replications to ensure high replication quality. Finally, microthermoforming of COC film is performed using a hot embossing machine (Wickert Maschinenbau) at 170°C (bottom) / 165°C (top) plus air pressure of 700 mbar (300 s) and 3000 mbar (600 s). Optionally, a stack of up to three 200 μm thick COC films as substrates is merged, resulting in a 600 μm thick thermoform part for enhanced mechanical robustness.

Step 2: A lithography process, e.g. photomask-based ultraviolet lithography or maskless interference lithography, generates a negative master with picoliter features which is transferred into silicon (Si) or nickel (Ni). From Si or Ni a positive PDMS master is cast, followed by hot embossing in a 200 μm COC film to replicate the features. The process is performed with the same hot embossing machine as in step 1, using the following process parameters: 160°C (bottom) / 180°C (top), plus air pressure of 200 mbar (200 s) and 3000 mbar (200 s).

Step 3: Finally, the two structured films are thermally sealed. By attaching the low-melting COC 8007 sides of both films (750 mbar for 60 s, followed by 1500 mbar for 5 s, both at 120 °C) in a modified hot embossing machine (Hex 01, JENOPTIK) a seal is created, while their outer high-melting COC 6013 sides ensure structural integrity. Further details on this process can be found in an earlier publication from our group [20].

2.2. Multi-scale microfluidic chip design

To demonstrate the fabrication concept, we designed a multi-scale microfluidic chip (Fig. 2). The top layer includes vents, pipetting ports, and chambers (up to 1500 μm feature size). The bottom layer features one of two designs: pyramidal microwell array (25 μm side length, 17 μm depth, 3.6 pl volume, 115,000 microwells/cm^2) or conical microwell array (20 μm diameter, 11 μm depth, 2.6 pl volume, 184,750 microwells/cm^2).

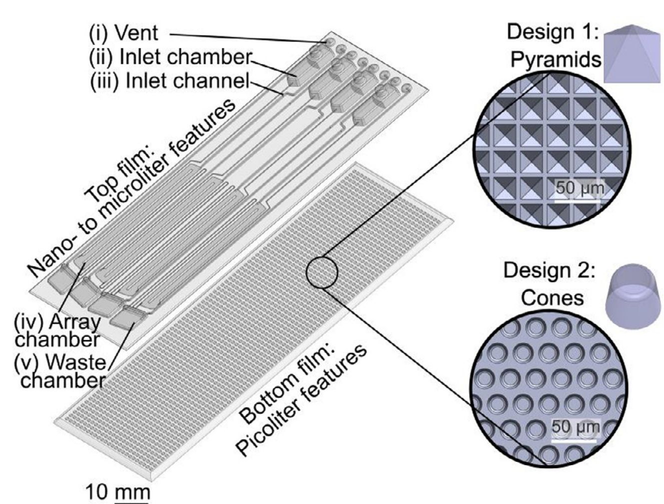

Fig. 2. The chip design consists of a top layer containing channels and chambers, and a bottom layer containing one of two exemplary picoliter-sized array features (pyramidal and conical microwells).

2.3. Chip characterization

The top layer was examined by confocal microscopy (TOOLinspect, Confovis) to verify dimensional accuracy (ESI Fig. S1-S2, Tab. S1). The bottom layer's picoliter features were characterized by scanning electron microscopy (SEM) (MAIA-3, TESCAN) (ESI Fig. S3). In microfluidic proof-of-concept experiments the picoliter microwells were filled with dPCR reagents and sealed with oil (ESI Tab. S2) Filling was carried out in a custom-made centrifuge (EULER 3.0, BioFluidix GmbH) and evaluated by fluorescence microscopy (Axio Observer Z1, Carl Zeiss) using either an object-slide or a disk-shaped layout (ESI Fig. S4, Tab. S3). Test of sealing strength was performed in a custom-made PCR-centrifuge (LabDisk Player 1, Dialunox).

3. Results

3.1. Characterization of nano- to microliter-features

Measurements using confocal microscopy confirmed that the desired dimensions were accurately replicated in the COC film (Table 1). Overall, we achieved a fabrication accuracy below ±10 µm and a coefficient of variation (CV) between 0.1 % and 3.1 % for feature sizes between 25 and 1500 µm. Details on the fabrication accuracy across the earlier processes of step 1 (PMMA micro-milling, PDMS casting and COC microthermoforming) can be found in the ESI (Tab. S1).

3.2. Characterization of picoliter-features

SEM images (Fig. 3a–d) taken after step 2 (hot embossing) showed successful transfer of patterns from the lithography masters in the COC films. The evaluation of pyramidal and conical features indicated minor deviations from the model, summarized in Table 1. These results demonstrate that the structural integrity of the picoliter patterns is largely maintained during the replication process. Post-sealing SEM images taken after step 3 revealed that the structural integrity of the patterns remained intact, though some thermal effects, in particular rounded edges, were visible. As an example, the side length of the pyramids changed from 26.4 ± 0.1 µm (before sealing) to 25.8 ± 0.4 µm (after sealing). For the conical wells, the bottom diameter shifted from 18.7 ± 0.1 µm to 19.1 ± 0.1 µm. Surface smoothening was also observed following thermal sealing, as seen in Fig. 3e–f. Cross-sectional SEM images before and after sealing of COC films with conical wells can be found in the ESI (Fig. S3).

3.3. Application demonstration

Utilizing a centrifugal microfluidic filling protocol (ESI Fig. S5, Tab. S4), we confirmed the microfluidic functionality. First, using stroboscopic microscopy imaging, we demonstrated microfluidic filling, draining and oil-sealing of the array chamber (ESI Fig. S7). Second, by imaging of fluorescent dPCR mix, we confirm robust and homogeneous filling of both picoliter microwell designs (Fig. 3g–h). Mechanical sealing strength was tested through centrifugal microfluidic experiments, where a liquid column inside the sealed device generated pressures of up to 1.85 bar at a rotational frequency of 60 Hz (ESI Eq. 1). The sealing remained intact even under prolonged heating times (up to 3 h, up to 95 °C).

4. Discussion

Our fabrication concept effectively decouples the production of different feature sizes within a multi-scale device, enabling independent design and optimization of picoliter and nano- to

Table 1
Exemplary dimensions of the fabricated multi-scale devices in COC film (N = 3).

Feature	CAD Model	Dimension before sealing (x ± s)	CV before sealing	Dimension after sealing	CV after sealing
(i) Vent (width)	300 µm	(302.0 ± 0.9) µm	0.3 %	–	–
(ii) Inlet chamber (depth)	1500 µm	(1496 ± 1.6) µm	0.1 %	–	–
(iii) Inlet channel (depth)	100 µm	(94.7 ± 0.5) µm	0.5 %	–	–
(iv) Array chamber (depth)	25 µm	(22.7 ± 0.7) µm	3.1 %	–	–
Pyramids (side length)	25 µm	(26.4 ± 0.1) µm	0.4 %	(25.8 ± 0.4) µm	1.6 %
Cones (diameter)	20 µm	(18.7 ± 0.1) µm	0.5 %	(19.1 ± 0.1) µm	0.5 %

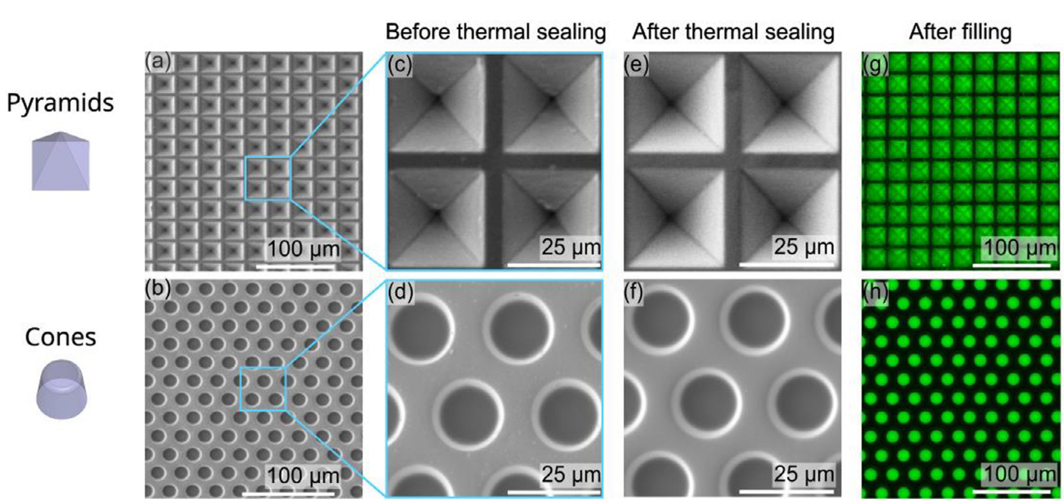

Fig. 3. SEM images of the picoliter-sized features in COC film before (c and d) and after (e and f) thermal sealing, confirming structural integrity throughout the procedure. Fluorescence images of pyramids (g) and cones (h) filled with dPCR mix.

microliter features. In contrast to an existing work, where sealing of 8 nm-sized features in thermoplastic films with minimal size change (±2 nm) was demonstrated [21], our fabrication and sealing approach does not require any surface treatment (e.g. plasma activation) [21–23] or additives (e.g. laser welding adsorbents) [2,24]. Aside from the cost of additional process steps, surface treatment can have a negative impact on the microfluidic functionality as well as on biomolecule adsorption behavior [21,22,25].

We achieved deviations from nominal CAD values below 10 μm for nano- to microliter features in microthermoformed COC films. Variations in measurements were mainly attributed to tolerances in micro-milling and shrinkage effects during PDMS curing and polymer film cooling, confirming earlier findings [12]. Such deviations of up to 10 μm are typically acceptable for larger features from 50 μm and highlight the need for complementary mastering processes for features below 25 to 50 μm. In the two investigated picoliter features, deviations from nominal values were below 2 μm, similar to previous findings on micropillar replications in COP plates [6]. This indicates improved accuracy compared to the nano- to microliter features. Our approach allows for seamless transitions between larger and smaller feature sizes.

Microfluidic experiments demonstrated strong sealing capabilities, even at temperatures up to 95 °C, suitable for demanding applications like PCR. Fluorescence imaging confirmed the microfluidic functionality of the microwells, despite observed surface smoothing during thermal sealing.

5. Conclusions

This work presents a novel method that allows affordable and scalable fabrication of patterned microstructures inside of microfluidic chips. It facilitates quick design iterations and reduces tooling costs while allowing early integration of product-grade thermoplastic materials, thus accelerating time-to-market and minimizing risks in development. The decoupling of picoliter and nano- to microliter feature fabrication enables the rapid production of complex geometries and high-density microstructures efficiently. Unlike many rapid prototyping techniques, our approach relies solely on COC material, avoiding non-scalable options like PDMS and eliminating the need for additives or surface treatments. This technology holds promise for diverse applications in multiscale lab-on-a-chip devices, including digital assays [2,7], integrated biomolecule extraction [5] and nanochannel sequencing [21].

Declaration of Generative AI and AI-assisted technologies in the writing process

During the preparation of this work the authors used ChatGPT (GPT-4o, OpenAI) in order to shorten the manuscript. After using this tool, the authors reviewed and edited the content as needed and take full responsibility for the content of the published article.

CRediT authorship contribution statement

Salman Murad: Writing – review & editing, Writing – original draft, Investigation, Formal analysis, Conceptualization. **Marvin Heyer:** Writing – review & editing, Writing – original draft, Methodology, Investigation, Formal analysis. **Fabian Lickert:** Writing – review & editing, Writing – original draft, Project administration, Investigation. **Judith Schlanderer:** Writing – review & editing, Investigation. **Daniel Kainz:** Writing – review & editing, Conceptualization. **Markus Rombach:** Writing – review & editing, Conceptualization. **Christoph Stöver:** Writing – review & editing, Investigation. **Thomas Ruhl:** Writing – review & editing, Investigation. **Benedikt Bläsi:** Writing – review & editing, Investigation. **Julian Menges:** Writing – review & editing, Methodology. **Tobias Hutzenlaub:** Writing – review & editing, Supervision, Funding acquisition. **Nils Paust:** Writing – review & editing, Supervision, Methodology, Funding acquisition. **Peter Juelg:** Writing – review & editing, Writing – original draft, Supervision, Project administration, Methodology, Funding acquisition, Conceptualization.

Declaration of competing interest

The authors declare that they have no known competing financial interests or personal relationships that could have appeared to influence the work reported in this paper.

Acknowledgments

We acknowledge the financial support of this work by the Federal Ministry of Education and Research (BMBF) within the projects EV-Surf (project number 13GW0605E) and OUTLIVE-CRC (project number 01KD2103C). We would further like to acknowledge the financial support by the Federal Ministry for Economic Affairs and Climate Action (BMWK) within the project MelB (IGF project no. 22486 N).

Appendix A. Supplementary data

Supplementary data to this article can be found online at https://doi.org/10.1016/j.mfglet.2025.07.005.

References

[1] Fu Y, Zhou H, Jia C, Jing F, Jin Q, Zhao J, et al. A microfluidic chip based on surfactant-doped polydimethylsiloxane (PDMS) in a sandwich configuration for low-cost and robust digital PCR. Sens Actuat B 2017;245:414–22. https://doi.org/10.1016/j.snb.2017.01.161.

[2] Kan CW, Rivnak AJ, Campbell TG, Piech T, Rissin DM, Mösl M, et al. Isolation and detection of single molecules on paramagnetic beads using sequential fluid flows in microfabricated polymer array assemblies. Lab Chip 2012;12(5):977–85. https://doi.org/10.1039/C2LC20744C.

[3] Sundberg SO, Wittwer CT, Gao C, Gale BK. Spinning disk platform for microfluidic digital polymerase chain reaction. Anal Chem 2010;82(4):1546–50. https://doi.org/10.1021/ac902398c.

[4] Campos CDM, Gamage SST, Jackson JM, Witek MA, Park DS, Murphy MC, et al. Microfluidic-based solid phase extraction of cell free DNA. Lab Chip 2018;18(22):3459–70. https://doi.org/10.1039/C8LC00716K.

[5] Schlenker F, Juelg P, Lüddecke J, Paust N, Zengerle R, Hutzenlaub T. Nanobead handling on a centrifugal microfluidic LabDisk for automated extraction of cell-free circulating DNA with high recovery rates. Analyst 2023;148(4):932–41. https://doi.org/10.1039/D2AN01820A.

[6] Kourmpetis I, Kastania AS, Ellinas K, Tsougeni K, Baca M, De Malsche W, et al. Gradient-temperature hot-embossing for dense micropillar array fabrication on thick cyclo-olefin polymeric plates: an example of a microfluidic chromatography column fabrication. Micro Nano Eng 2019;5:100042. https://doi.org/10.1016/j.mne.2019.100042.

[7] Podbiel D, Laermer F, Zengerle R, Hoffmann J. Fusing MEMS technology with lab-on-chip: nanoliter-scale silicon microcavity arrays for digital DNA quantification and multiplex testing. Microsyst Nanoeng 2020;6(1):82. https://doi.org/10.1038/s41378-020-00187-1.

[8] Chantiwas R, Park S, Soper SA, Kim BC, Takayama S, Sunkara V, et al. Flexible fabrication and applications of polymer nanochannels and nanoslits. Chem Soc Rev 2011;40(7):3677. https://doi.org/10.1039/c0cs00138d.

[9] Yang Y, Kulangara K, Sia J, Wang L, Leong KW. Engineering of a microfluidic cell culture platform embedded with nanoscale features. Lab Chip 2011;11(9):1638. https://doi.org/10.1039/c0lc00736f.

[10] Li Q, Jiang B, Li X, Zhou M. Investigation of solvent-assisted in-mold bonding of cyclic olefin copolymer (COC) microfluidic chips. Micromachines 2022;13(6):965. https://doi.org/10.3390/mi13060965.

[11] Utko P, Persson F, Kristensen A, Larsen NB. Injection molded nanofluidic chips: fabrication method and functional tests using single-molecule DNA experiments. Lab Chip 2011;11(2):303–8. https://doi.org/10.1039/C0LC00260G.

[12] Focke M, Kosse D, Müller C, Reinecke H, Zengerle R, Von Stetten F. Lab-on-a-foil: microfluidics on thin and flexible films. Lab Chip 2010;10(11):1365. https://doi.org/10.1039/c001195a.

[13] Jena RK, Yue CY, Lam YC, Wang ZY. High fidelity hot-embossing of COC microdevices using a one-step process without pre-annealing of polymer

substrate. Sens Actuat. B 2010;150(2):692–9. https://doi.org/10.1016/j.snb.2010.08.018.

[14] Metwally K, Robert L, Queste S, Gauthier-Manuel B, Khan-Malek C. Roll manufacturing of flexible microfluidic devices in thin PMMA and COC foils by embossing and lamination. Microsyst Technol 2012;18(2):199–207. https://doi.org/10.1007/s00542-011-1358-z.

[15] Scott S, Ali Z. Fabrication methods for microfluidic devices: an overview. Micromachines 2021;12(3):319. https://doi.org/10.3390/mi12030319.

[16] Strohmeier O, Keller M, Schwemmer F, Zehnle S, Mark D, von Stetten F, et al. Centrifugal microfluidic platforms: advanced unit operations and applications. Chem Soc Rev 2015;44(17):6187–229. https://doi.org/10.1039/C4CS00371C.

[17] Schlenker F, Kipf E, Borst N, Paust N, Zengerle R, Von Stetten F, et al. Centrifugal microfluidic integration of 4-Plex ddPCR demonstrated by the quantification of cancer-associated point mutations. Processes 2021;9(1):97. https://doi.org/10.3390/pr9010097.

[18] Aghvami SA, Opathalage A, Zhang ZK, Ludwig M, Heymann M, Norton M, et al. Rapid prototyping of cyclic olefin copolymer (COC) microfluidic devices. Sens Actuat B 2017;247:940–9. https://doi.org/10.1016/j.snb.2017.03.023.

[19] Steigert J, Haeberle S, Brenner T, Müller C, Steinert CP, Koltay P, et al. Rapid prototyping of microfluidic chips in COC. J Micromech Microeng 2007;17(2):333–41. https://doi.org/10.1088/0960-1317/17/2/020.

[20] Kosse D, Schwemmer F, Buselmeier D, Zengerle R, Von Stetten F. 3D Microfluidic Cartridges by Gas Pressure Assisted Thermal Bonding of Microthermoformed Films. In *2013 Transducers & Eurosensors XXVII: The 17th International Conference on Solid-State Sensors, Actuators and Microsystems (TRANSDUCERS & EUROSENSORS XXVII)*; IEEE: Barcelona, Spain, 2013; pp 1318–1321. https://doi.org/10.1109/transducers.2013.6627019.

[21] Rathnayaka C, Chandrosoma IA, Choi J, Childers K, Chibuike M, Akabirov K, et al. Detection and identification of single ribonucleotide monophosphates using a dual in-plane nanopore sensor made in a thermoplastic *via* replication. Lab Chip 2024;24(10):2721–35. https://doi.org/10.1039/D3LC01062G.

[22] Roy S, Yue CY. Surface modification of COC microfluidic devices: a comparative study of nitrogen plasma treatment and its advantages over argon and oxygen plasma treatments. Plasma Process Polym 2011;8(5):432–43. https://doi.org/10.1002/ppap.201000120.

[23] Wu J, Chantiwas R, Amirsadeghi A, Soper SA, Park S. Complete plastic nanofluidic devices for DNA analysis via direct imprinting with polymer stamps. Lab Chip 2011;11(17):2984. https://doi.org/10.1039/c1lc20294d.

[24] Jonušauskas L, Rekštytė S, Buivydas R, Butkus S, Paipulas D, Gadonas R, Juodkazis S, Malinauskas M. Laser Subtractive-Additive-Welding Microfabrication for Lab-On-Chip (LOC) Applications; Von Freymann, G., Schoenfeld, W. V., Rumpf, R. C., Eds.; San Francisco, California, United States, 2017; p 101150V. https://doi.org/10.1117/12.2249828.

[25] Kitsara M, Ducrée J. Integration of functional materials and surface modification for polymeric microfluidic systems. J Micromech Microeng 2013;23(3):033001. https://doi.org/10.1088/0960-1317/23/3/033001.